Colloid Polym Sci (2007) 285:999–1007
DOI 10.1007/s00396-007-1645-5

ORIGINAL CONTRIBUTION

Drying dissipative patterns of biological polyelectrolyte solutions

Tsuneo Okubo · Daisuke Onoshima · Akira Tsuchida

Received: 31 October 2006 / Accepted: 26 December 2006 / Published online: 7 February 2007

Abstract Drying dissipative structural patterns of aqueous solutions of biological polyelectrolytes, sodium poly (α, *L*-glutamate; NaPGA) and poly (-*L*-lysine hydrobromide; PLL.HBr), were studied on a cover glass. Below the critical polymer concentration, *m** (ca. 0.003 and ca. 0.01 monoM for NaPGA and PLL.HBr, respectively), the dried patterns shrank only around the center of the initial solution area wetted on a cover glass. Above the *m** values, on the other hand, the drying pattern extended throughout the initial solution area. The *m** values agreed excellently with the critical polymer concentrations, where the surface tensions started to decrease sharply as the polymer concentrations increased. The broad rings were always observed in the drying patterns of any solutions examined. The spoke-like cracks appeared at the polymer concentrations above the *m** values and only in the area of the broad rings. Microscopic structures such as cross-like, rod-like, and block-like patterns formed irrespective of polymer concentrations. Especially, the city-road-like microscopic pattern was observed for PLL.HBr solutions, which strongly supports the formation of crystal structures of PLL.HBr that remain in the whole processes of dryness. These patterns were correlated deeply with the crystal-like orientation of the biological polyelectrolytes at the air–solution interfaces.

Keywords Drying dissipative structure · Sodium poly (α, *L*-glutamate) · Poly (-*L*-lysine hydrobromide) · Broad ring · Spoke-like crack Crystal-like orientation at interface

T. Okubo (✉)
Institute for Colloidal Organization,
Hatoyama 3-1-112,
Uji, Kyoto 611-0012, Japan
e-mail: okubotsu@ybb.ne.jp

T. Okubo
Cooperative Research Center, Yamagata University,
Johnan 4-3-16,
Yonezawa 992-8510, Japan

D. Onoshima · A. Tsuchida
Department of Applied Chemistry, Gifu University,
Gifu 501-1193, Japan

Introduction

Generally speaking, most structural patterns in nature form via self-organization accompanied with the dissipation of free energy and in the nonequilibrium state. Among several factors in the free energy dissipation of aqueous colloidal suspensions, evaporation of water molecules at the air–water interface and the gravitational convection are very important. To understand the mechanisms of the dissipative self-organization of the simple model systems instead of the much complex nature itself, the authors have studied the *convectional*, *sedimentation*, and *drying* dissipative patterns of colloidal suspensions as systematically as possible.

Drying dissipative patterns have been studied for suspensions and solutions of many kinds of solutes, colloidal particles [1–13], linear-type polyelectrolytes [14], water-soluble nonionic polymers [15, 16], ionic and nonionic detergents [17–19], and gels [20] mainly on a cover glass. The macroscopic broad-ring patterns of the hill accumulated with spheres in the outside edges always formed. For the nonspherical particles, the round hill was formed in the center area in addition to the broad ring. Macroscopic spoke-like cracks or fine hills including flickering spoke-like ones were also observed for many solutes. The convection of water and solute molecules at different rates under gravity and the translational and rotational Brownian movement of

the latter were important for the macroscopic pattern formation. Furthermore, beautiful fractal patterns such as branch-like, arc-like, block-like, star-like, cross-like, and string-like ones were observed in the microscopic scale. These microscopic drying patterns were reflected from the *shape*, *size*, and *flexibility* of the solute molecules themselves. Microscopic patterns also formed the electrostatic and hydrophobic interactions between solutes and/or between the solutes and substrate in the course of solidification. A very important finding in our experiments was that the primitive vague patterns were already formed in the concentrated suspension state before dryness and grew toward fine structures in the course of solidification.

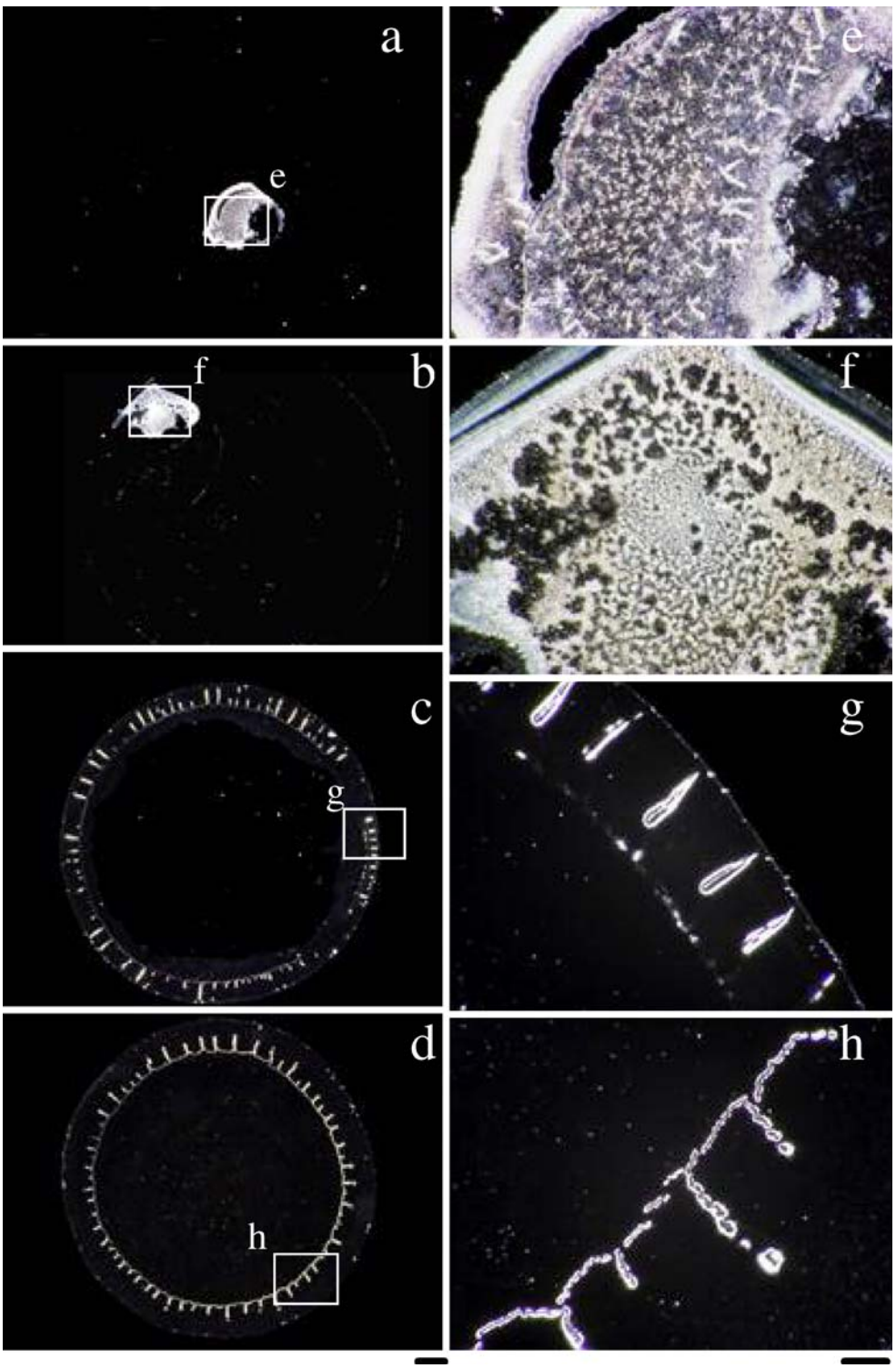

Fig. 1 Drying dissipative patterns of NaPGA solution on an unrinsed cover glass at 25 °C. In water, 0.1 ml: **a**, **e** 1×10^{-5} monoM; **b**, **f** 1×10^{-3} monoM; **c**, **g** 0.01 monoM; **d**, **h** 0.03 monoM; length of the bar is 1.0 mm (**a**–**d**), 0.2 mm (**e**–**h**)

Quite recently, the *sedimentation* dissipative patterns have been studied in the course of drying suspensions of colloidal silica spheres and green tea in a glass dish, a watch glass, and others [21–23]. The broad-ring patterns were formed within 10 min in the suspension state by the convectional flow of water and colloidal particles. The important finding was that the sedimentary particles were suspended above the substrate and always moved by the external fields including convectional flow and the sedimentation of the particles by gravity.

The *Convectional* dissipative structures were studied for Chinese black ink and the 100% ethanol suspensions of colloidal silica spheres in our laboratory [10, 24]. The existence of the small circle-like *convection cells* proposed by Terada et al. [25–28], for the first time, was supported. A vigorous cell convectional flow was observed for the suspensions with the naked eye, and the patterns changed dynamically with time.

In this work, drying dissipative patterns of the typical biological polyelectrolytes, i.e., sodium poly (α, *L*-glutamate; NaPGA) and poly (*L*-lysine hydrobromide; PLL.HBr), have been observed on a cover glass. These polymers are highly monodisperse in their molecular weights and regular in their conformations of polymer chains. Characteristic macroscopic and microscopic patterns appeared. These patterns were correlated deeply with the conformations of the polyelectrolytes at the air–solution interfaces.

Experimental

Materials

NaPGA (molecular weight (*MW*)=15,000–50,000) and PLL.HBr (*MW*=1,000–4,000) were purchased from Sigma-Aldrich Japan (Tokyo) and Wako Pure Chemicals (Tokyo), respectively. The water used for the sample purification and preparation was purified by a Milli-Q reagent grade system (Milli-RO5 plus and Milli-Q plus, Millipore, Bedford, MA).

Observation of the dissipative structures

0.1 ml of the polyelectrolyte solutions were dropped carefully and gently on a micro cover glass (30×30 mm, thickness no. 1, 0.12–0.17 mm; Matsunami Glass, Kishiwada, Osaka) set in a glass dish (60 mm in diameter, 15 mm in depth; Petri, Tokyo). The cover glasses were used without further rinsing and rinsed after with chromic–sulfuric acid mixture for 24 h. The contact angles for the pure water were 11±0.5° and 31±0.5° from the drop profiles of water on the unrinsed and rinsed cover glasses, respectively. Extrapolation to the zero amount of water was made from the measurements with several amounts of water. Disposable serological pipettes (1.0 ml, Corning Lab. Sci.) were used for the dropping solutions. An observation of the macroscopic and microscopic drying patterns was made for the film formed after the suspension

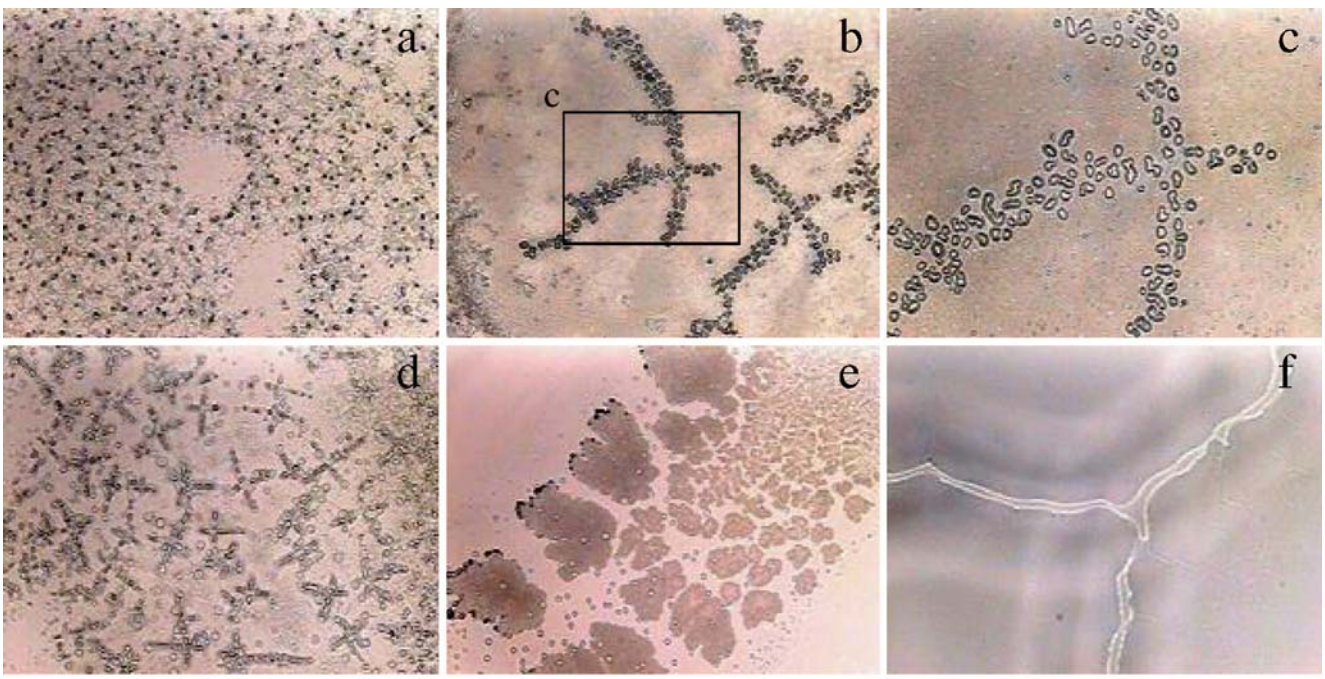

Fig. 2 Drying dissipative patterns of NaPGA solution on an unrinsed cover glass at 25 °C. In water, 0.1 ml: **a** 1×10^{-7} monoM; **b**, **c** 1×10^{-5} monoM; **d**, **e** 1×10^{-4} monoM; **f** 0.01 monoM; length of the bar is 0.1 mm (**b**), 0.04 mm (**a**, **c**–**f**)

was dried up completely on a cover glass in a room air-conditioned at 25 °C and 50–60% in humidity. Concentrations of the polymers ranged from 1×10^{-7} to 0.03 monoM.

Macroscopic and microscopic dissipative patterns were observed with a digital HD microscope (type VH-7000, Keyence, Osaka) and a laser digital microscope (type VH-8500, Keyence). Macroscopic close-up pictures were also taken with a Canon EOS 100QD camera with a macro-lens (EF 50 mm, f=2.5) and a life-size converter EF.

Surface tension measurements

Surface tension was measured on a Wilhelmy-type surface tensiometer (type ST-1, New Version, Shimadzu, Kyoto) [29]. A ground glass measuring plate was suspended from an

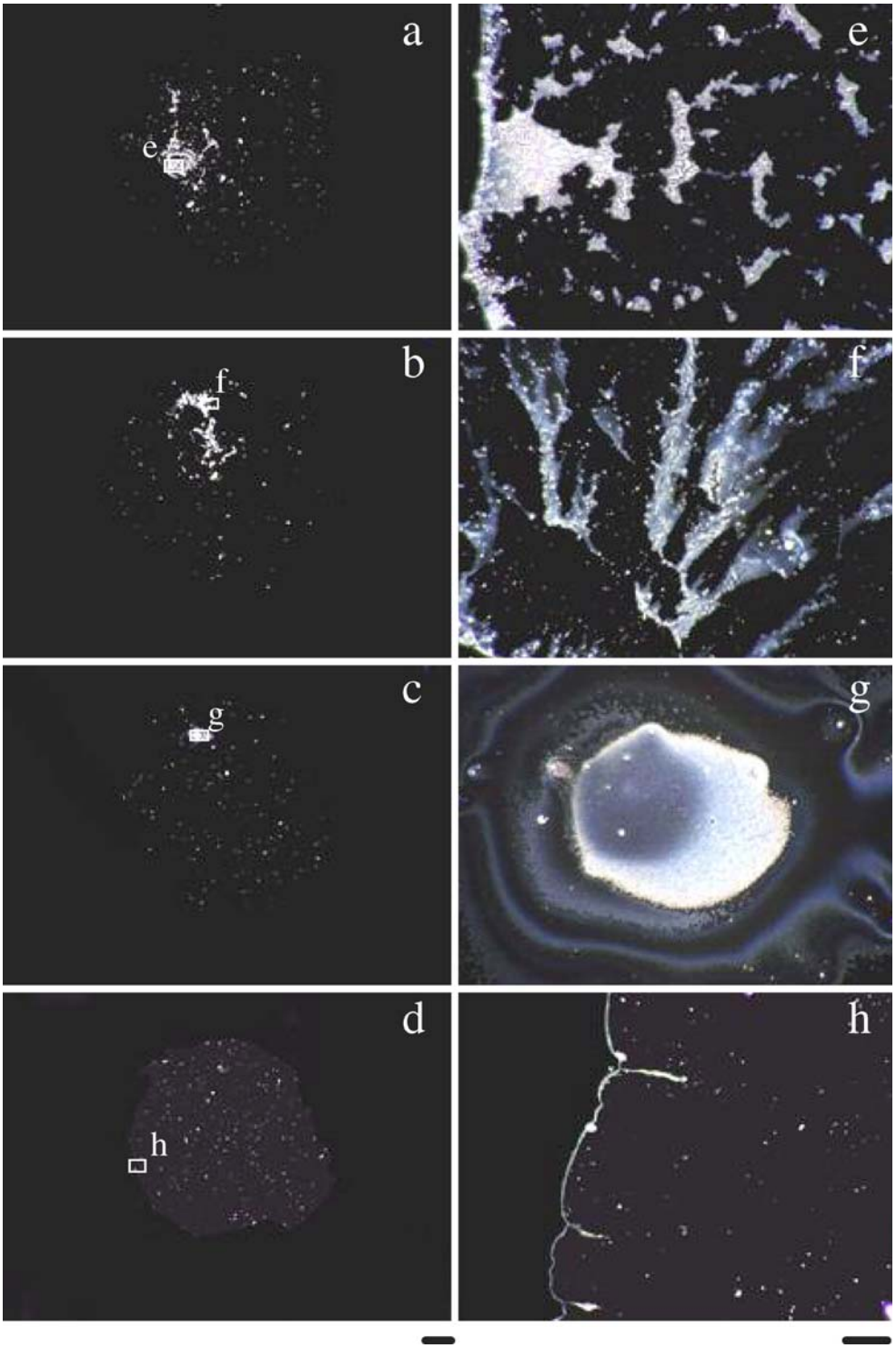

Fig. 3 Drying dissipative patterns of NaPGA solution on a rinsed cover glass at 25 °C. In water, 0.1 ml: **a**, **e** 1×10^{-7} monoM; **b**, **f** 1×10^{-5} monoM; **c**, **g** 1×10^{-3} monoM; **d**, **h** 0.01 monoM; length of the bar is 3.0 mm (**a**–**d**), 0.2 mm (**e**–**h**)

electrobalance into the sample solution in a glass dish, the inner diameter of which was 40 mm. The measurements were made at room temperature regulated at 25±0.5 °C. The cell room of the tensiometer was saturated with water vapor during the measurements to avoid dryness of the measuring plate and evaporation of the sample solution. It takes from 30 min to 8 h before the equilibrium values of the surface tension are obtained. The experimental errors of our surface tension measurements are estimated to be 3 N/m.

Results and discussion

Drying dissipative patterns of NaPGA solutions

Figure 1 shows the typical drying patterns of NaPGA at concentrations ranging from 1×10^{-5} to 0.03 monoM on an unrinsed cover glass. The right-hand side pictures (Fig. 1e–h) are extended pictures of the corresponding ones at the squares left-hand side (Fig. 1a–d). Surprisingly, when the initial polymer concentrations were lower than the critical concentration, m^* (ca. 0.003 monoM), the drying patterns of NaPGA solutions shrank around the center of the initial solution area. Above the m^*, on the other hand, the dried film extended in the full area of the initial solution drop on an unrinsed cover glass. The main cause for this characteristic concentration dependency of the pattern areas was clarified to be the change in the surface activity of the NaPGA solution at the air–solution interface as discussed in detail below using Fig. 4.

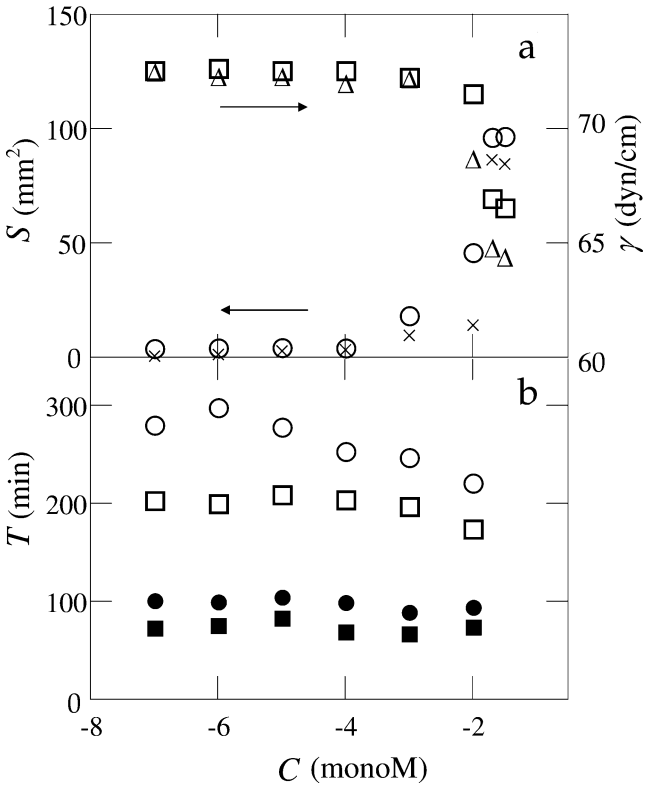

Fig. 4 Area (S), drying time (T), and surface tension (γ) of NaPGA and PLL.HBr as a function of polymer concentration at 25 °C. In water, 0.1 ml: **a** *open circles*, NaPGA; *times symbols*, PLL.HBr; *open triangles*, NaPGA, pH=6.0–7.7; *open squares*, PLL.HBr, pH=2.5–5.8; **b** *open circles*, NaPGA, unrinsed; *open squares*, PLL.HBr, unrinsed; *closed circles*, NaPGA, rinsed; *closed squares*, PLL.HBr, rinsed

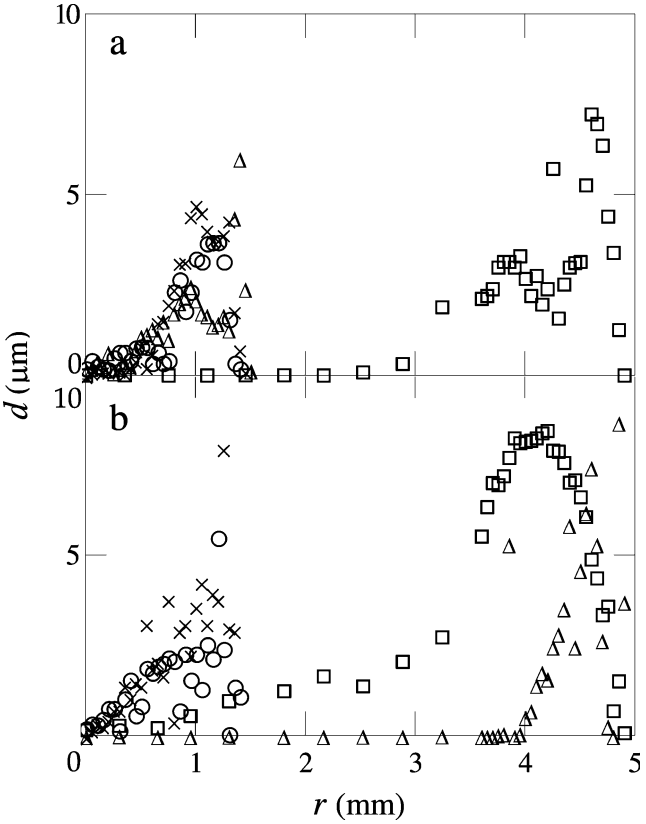

Fig. 5 Thickness (d) of the dried film of NaPGA (**a**) and PLL.HBr (**b**) on an unrinsed cover glass as a function of radius (r) at 25 °C. In water, 0.1 ml: **a** *open circles*, 1×10^{-7} monoM; *times symbols*, 1×10^{-5} monoM; *open triangles*, 1×10^{-3} monoM; *open squares*, 0.01 monoM; **b** *open circles*, 1×10^{-7} monoM; *times symbols*, 1×10^{-5} monoM; *open triangles*, 0.01 monoM; *open squares*, 0.03 monoM

The broad rings shown by white circles at the outer edges were observed for all the pictures in Fig. 1. A main cause for the broad-ring formation is because of the convectional flow of water and the polyelectrolyte solutes in different rates, where the rate of the latter is slower than that of the former under gravity. Especially, flow of the solutes from the center area toward the outside edges in the lower layers of the liquid drop, which was observed on a digital HD microscope directly from the movement of the very rare occurring aggregates of the colloidal particles of Chinese black ink, is important [10]. It should be noted that the broad-ring formation has been observed for all the solutions and suspensions examined by our group [7–14, 16–24] and further by other researchers [1–6]. Recently,

microgravity experiments were made for the observation of drying dissipative patterns of the deionized suspension of colloidal silica spheres [30]. Surprisingly, the broad-ring patterns did not disappear even in microgravity. This supports the idea that both gravitational and Marangoni convections contribute to the broad-ring formation on the earth, but the latter is still important in microgravity.

Figure 2 shows the typical examples of the most extended drying patterns for NaPGA on an unrinsed cover glass, where lengths of the full scales are 40 or 100 μm. When the polymer concentrations were very low at 1×10^{-7} and 1×10^{-6} monoM, the microscopic patterns in the center areas surrounded with the broad rings were block-like and/or bead-like structures (see Fig. 2a for example). At 10^{-5} monoM, many of the microscopic patterns' inner area

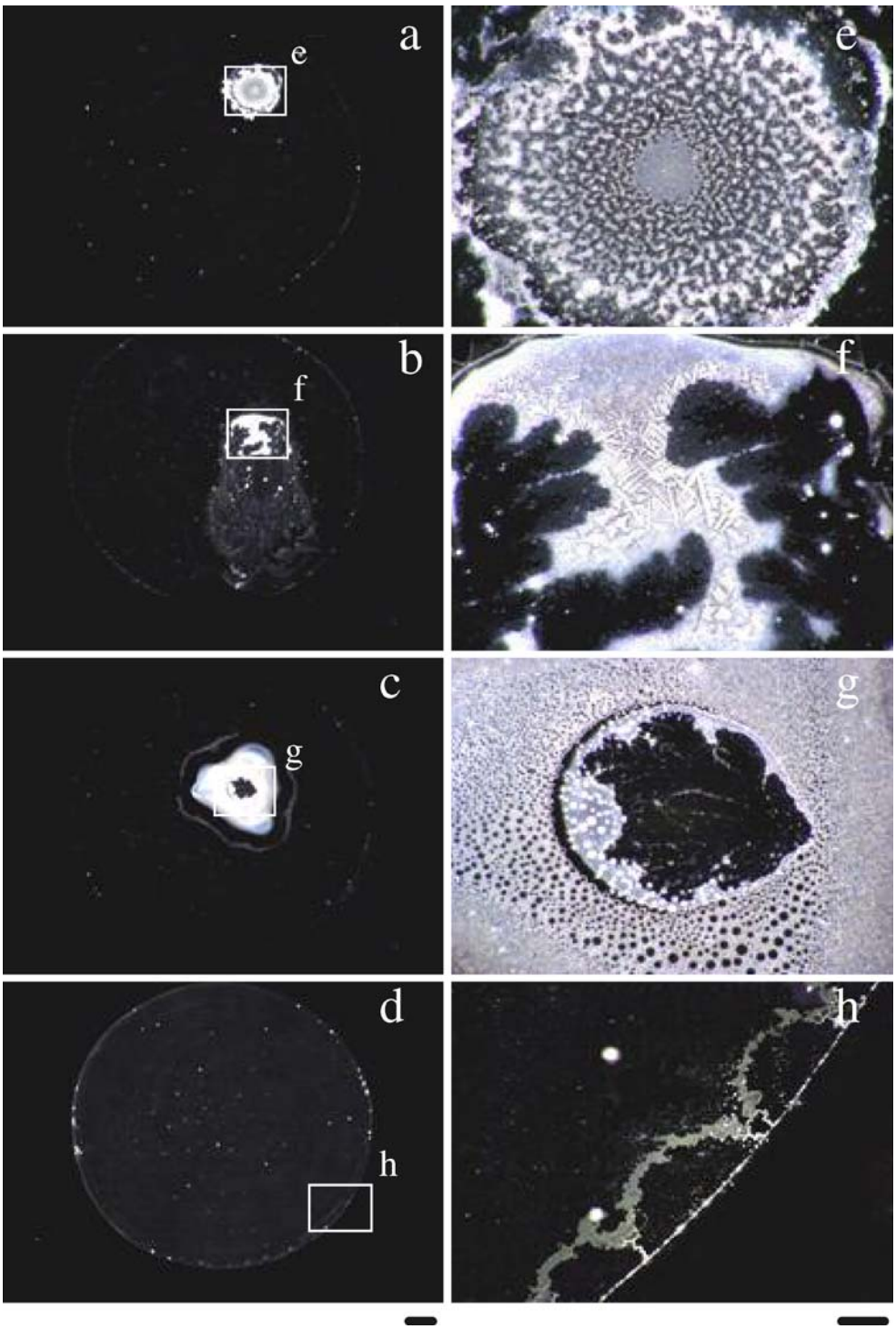

Fig. 6 Drying dissipative patterns of PLL.HBr solution on an unrinsed cover glass at 25 °C. In water, 0.1 ml: **a**, **e** 1×10^{-7} monoM; **b**, **f** 1×10^{-5} monoM; **c**, **g** 1×10^{-3} monoM; **d**, **h** 0.03 monoM; length of the bar is 1.0 mm (**a**–**d**), 0.2 mm(**e**–**h**)

surrounded with the broad rings were like crosses composed of bead-like blocks as seen in Fig. 2b–d. When the concentration was 1×10^{-4} monoM, the crosses composed of the bead-like blocks and lagoon-like islands coexisted. The lagoon-like structures became major among the microscopic patterns at 1×10^{-3} monoM in the NaPGA concentration. Above the critical concentration, m^*, microscopic patterns were spoke-like cracks only in the broad-ring areas and composed of the flickering curves or circles as shown in Fig. 1c,d,g,h.

Figure 3 shows the drying patterns of NaPGA on a rinsed cover glass. The areas of the film on a rinsed cover glass extended significantly compared with those on an unrinsed cover glass. Furthermore, the patterns on a rinsed cover glass were different from those on an unrinsed cover glass. Interestingly, the patterns were also roughly grouped below and above the critical concentration, m^*, at ca. 0.003 monoM; that is, the pattern areas also shrank or extended below or above the m^* value. It should be noted here that the convectional flow is enhanced by the evaporation of water at the air–liquid interface, resulting in the lowering of the suspension temperature in the upper region. When the polymers reach the edges of the drying frontier at the outside region of the liquid, a part of the polymer solutes will turn upward and go back to the center region. However, the movement of most solutes may stop at the frontier region by the disappearance of water. This process must be followed by the broad-ring accumulation of the particles near the round edges. It should be noted here that the main cause for the patterns observed here is the convectional flows of polymer solutes and water with different rates, respectively.

Figure 4a shows the area S of the dried film and the surface tension γ of the corresponding initial solutions of NaPGA as a function of polymer concentration; although those of PLL.HBr are also shown in Fig. 4b. Clearly, S and γ turned to increase and decrease above the NaPGA concentration around 0.003 monoM corresponding m^*. As discussed by one of the authors previously [28], biological polyelectrolytes including sodium chondroitin sulfates A and C, NaPGA, PLL.HBr, deoxyribonucleic acid, lysozyme, and bovine serum albumin had no surface activity below the critical polymer concentration, m^*, but increased as the concentration increased above m^*. Furthermore, the high surface activity was accompanied with the orientation of the polyelectrolytes along the air–water interface [28]. Separation into the hydrophobic and hydrophilic moieties at the interface and balance in their strength were important for the appearance of the surface activity. The m^* values were around 0.003 and 0.01 for the solutions of NaPGA and PLL.HBr, respectively. Thus, the concentration dependencies of S values are explained nicely with the change in the surface activities at the air–glass interfaces. Figure 4a also shows the S and γ values for PLL.HBr, where m^* was ca. 0.01 monoM. The quite similar concentration dependence of S as NaPGA was also observed.

Figure 4b shows the drying time of NaPGA and PLL.HBr as a function of their concentrations. The T values

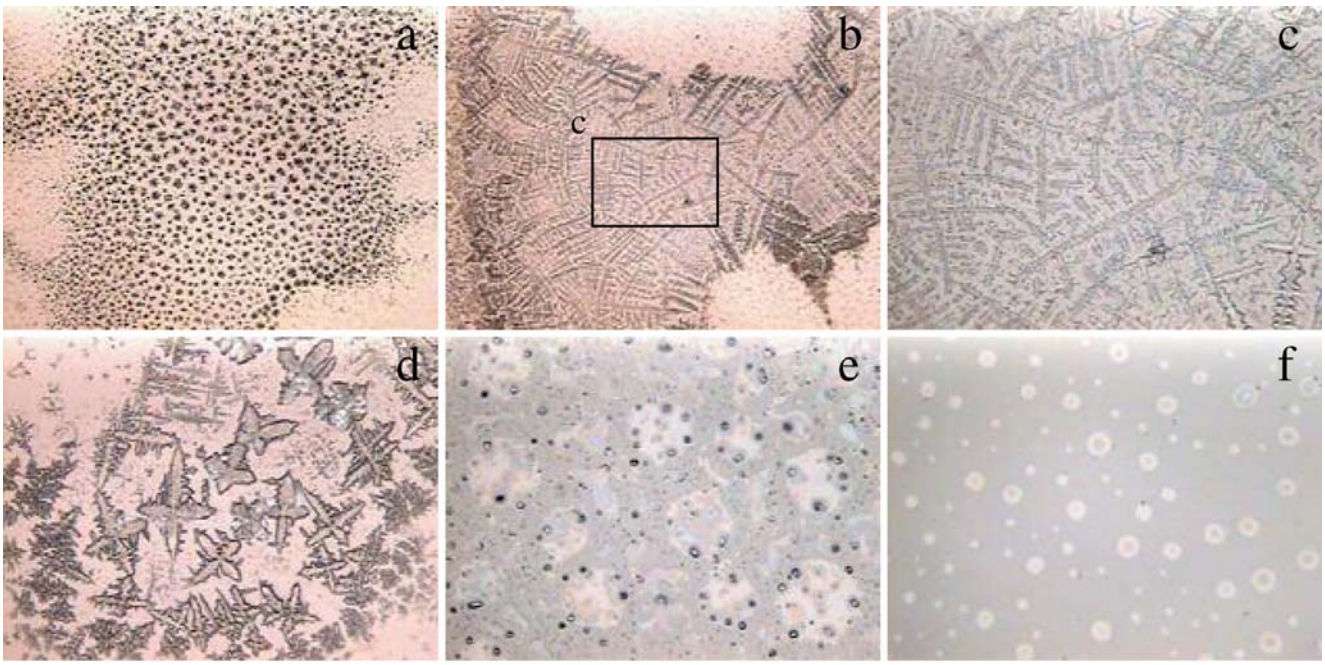

Fig. 7 Drying dissipative patterns of PLL.HBr solution on an unrinsed cover glass at 25 °C. In water, 0.1 ml: **a** 1×10^{-5} monoM; **b**, **c**, **d** 1×10^{-4} monoM; **e** 1×10^{-3} monoM; **f** 0.01 monoM; length of the bar is 0.1 mm (**b**), 0.04 mm (**a**, **d**, **e**, **f**), 0.02 mm (**c**)

seem to decrease transitionally also above m^*, 0.003 and 0.01 monoM for NaPGA and PLL.HBr, respectively; although the experimental errors were rather high. These observations are also consistent with the fact that the extended liquids with high surface activity on a cover glass dried much faster compared with the shrunken liquid drops with very low surface activity.

Figure 5a shows the thickness of the film (d) as a function of the distance from the center (r) for NaPGA solutions at concentrations ranging from 1×10^{-7} to 0.01 monoM. The d values were measured directly using a laser 3D profile microscope. The rather large experimental errors in the d values are clear, but the d–r profiles shown in Fig. 5a support the existence of the broad-ring patterns; although the shoulders often exist beside the broad

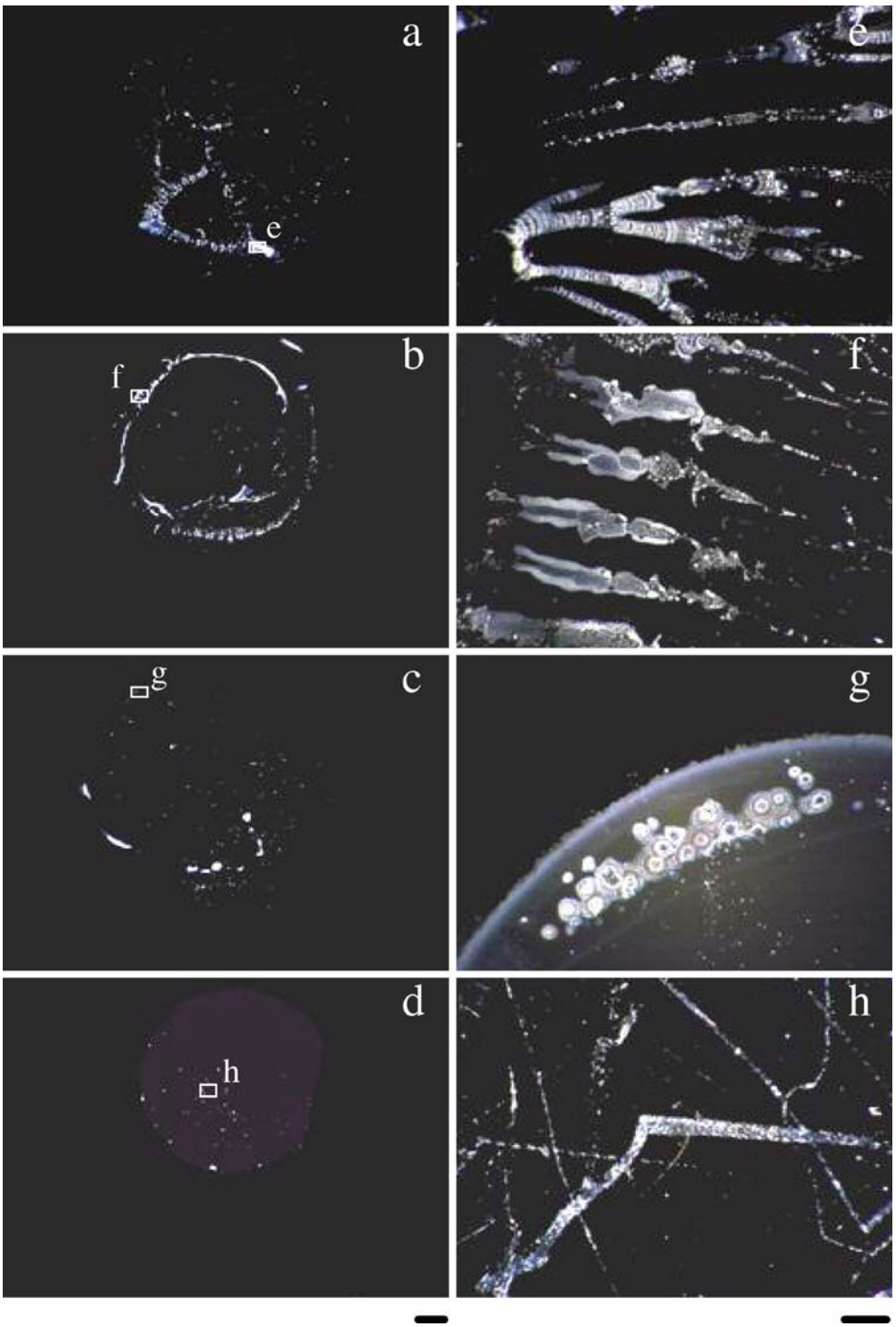

Fig. 8 Drying dissipative patterns of PLL.HBr solution on a rinsed cover glass at 25 °C. In water, 0.1 ml: **a**, **e** 1×10^{-7} monoM; **b**, **f** 1×10^{-4} monoM; **c**, **g** 1×10^{-3} monoM; **d**, **h** 0.01 monoM; length of the bar is 3.0 mm (**a**–**d**), 0.2 mm (**e**–**h**)

rings. It should be recalled that the central region of the film of the spherical particles was always extremely thin as was often observed hitherto [7, 8, 11].

Drying dissipative patterns of PLL.HBr solutions

Figure 6 shows the typical drying patterns of PLL.HBr on a rinsed cover glass at polymer concentrations of 1×10^{-7}, 1×10^{-5}, 1×10^{-3}, and 0.03 monoM. Shrinking of the drying pattern area took place below m^*, ca. 0.01 monoM. Above m^* (see Fig. 6d), on the other hand, the area increased transitionally. This observation also demonstrates that the ordered structure, where the nonpolar and polar moieties at the air–water interface split, took place for the PLL.HBr system [28]. Clearly, broad rings were observed in the drying patterns irrespective of polymer concentrations. In the inner area of the broad ring below m^*, various types of microscopic patterns were observed. Most of the extended structures are shown in Fig. 7. Bead-like and block-like patterns were observed especially at low polymer concentrations. It should be mentioned here that the city-road-like patterns were often observed (see Fig. 7b–d). This pattern strongly supports the idea that crystallization took place in the course of solidification. Crystallization is highly plausible, as the crystal-like ordered structures at the air–solution interface remain in the whole course of dryness. Relating this structure, similar city-road-type patterns were observed in the drying processes of ethanol and/or methanol solutions of fluorescent dyes such as 7-amino-4-trifluoromethyl coumarin (Okubo T, Yokota N, Tsuchida A, unpublished results).

Figure 8 shows the typical patterns of PLL.HBr on a rinsed cover glass. Shrunken and extended areas were observed below and above the critical concentration, $m^*=$ 0.01 monoM; although the pictures in Fig. 8a–d do not show clearly the distinction between the shrunken and extended areas. Surprisingly, the patterns observed for PLL.HBr are quite similar to those of NaPGA. This work strongly supports the existence of the ordered crystal-like structures at the air–solution interface, which has been clarified from the surface tension measurements before [29].

Acknowledgment Financial supports from the Ministry of Education, Culture, Sports, Science and Technology, Japan and Japan Society for the Promotion of Science are greatly acknowledged for Grants-in-Aid for Exploratory Research (17655046) and Scientific Research (B; 18350057), respectively. Catalysts and Chemicals is thanked deeply for providing the colloidal silica sphere samples used in this work.

References

1. Vanderhoff JW (1973) J Polym Sci Polym Symp 41:155
2. Nicolis G, Prigogine I (1977) Self-organization in non-equilibrium systems. Wiley, New York
3. Ohara PC, Heath JR, Gelbart WM (1997) Angew Chem 109:1120
4. Maenosono S, Dushkin CD, Saita S, Yamaguchi Y (1999) Langmuir 15:957
5. Nikoobakht B, Wang ZL, El-Sayed MA (2000) J Phys Chem 104:8635
6. Ung T, Litz-Marzan LM, Mulvaney P (2001) J Phys Chem B 105:3441
7. Okubo T, Okuda S, Kimura H (2002) Colloid Polym Sci 280:454
8. Okubo T, Kimura K, Kimura H (2002) Colloid Polym Sci 280:1001
9. Okubo T, Kanayama S, Kimura K (2004) Colloid Polym Sci 282:486
10. Okubo T, Kimura H, Kimura T, Hayakawa F, Shibata T, Kimura K (2005) Colloid Polym Sci 283:1
11. Okubo T, Yamada T, Kimura K, Tsuchida A (2005) Colloid Polym Sci 283:1007
12. Yamaguchi T, Kimura K, Tsuchida A, Okubo T, Matsumoto M (2005) Colloid Polym Sci 283:1123
13. Okubo T, Nozawa M, Tsuchida A (2006) Colloid Polym Sci (in press). DOI 10.1007/s00396-006-1626-0
14. Okubo T, Kanayama S, Ogawa H, Hibino M, Kimura K (2004) Colloid Polym Sci 282:230
15. Shimomura M, Sawadaishi T (2001) Curr Opin Colloid Interface Sci 6:11
16. Okubo T, Yamada T, Kimura K, Tsuchida A (2006) Colloid Polym Sci 284:396
17. Okubo T, Kanayama S, Kimura K (2004) Colloid Polym Sci 282:486
18. Kimura K, Kanayama S, Tsuchida A, Okubo T (2005) Colloid Polym Sci 283:898
19. Okubo T, Shinoda C, Kimura K, Tsuchida A (2005) Langmuir 21:9889
20. Okubo T, Itoh E, Tsuchida A, Kokufuta E (2006) Colloid Polym Sci 285:339
21. Okubo T (2006) Colloid Polym Sci 284:1395
22. Okubo T (2006) Colloid Polym Sci 284:1191
23. Okubo T (2006) Colloid Polym Sci 285:331
24. Okubo T (2006) Colloid Polym Sci 285:225
25. Terada T, Yamamoto R, Watanabe T (1934) Sci Paper Inst Phys Chem Res Jpn 27:173
26. Terada T, Yamamoto R, Watanabe T (1934) Proc Imper Acad Tokyo 10:10
27. Terada T, Yamamoto R, Watanabe T (1934) Sci Paper Inst Phys Chem Res Jpn 27:75
28. Terada T, Yamamoto R (1935) Proc Imper Acad Tokyo 11:214
29. Okubo T, Kobayashi K (1998) J Colloid Interface Sci 205:433
30. Tsuchida A, Okubo T (2003) Sen'I Gakkaishi 59:264